Biosensors and Bioelectronics 91 (2017) 246–252

Contents lists available at ScienceDirect

Biosensors and Bioelectronics

journal homepage: www.elsevier.com/locate/bios

A novel immunosensing platform for highly sensitive prostate specific antigen detection based on dual-quenching of photocurrent from CdSe sensitized TiO_2 electrode by gold nanoparticles decorated polydopamine nanospheres

Yu-Xiang Dong[a,b], Jun-Tao Cao[a,b,*], Yan-Ming Liu[a,b,*], Shu-Hui Ma[c]

[a] College of Chemistry and Chemical Engineering, Xinyang Normal University, Xinyang 46400, China
[b] Institute for Conservation and Utilization of Agro-bioresources in Dabie Mountains, Xinyang Normal University, Xinyang 464000, China
[c] Xinyang Central Hospital, Xinyang 464000, China

ARTICLE INFO

Keywords:
Dual quenching strategy
AuNPs-Dpa-melanin CNSs
Photoelectrochemical biosensor
Exciton energy transfer
Steric hindrance effect
Prostate specific antigen

ABSTRACT

Herein, a novel photoelectrochemical (PEC) immunosensing platform for highly sensitive detection of prostate specific antigen (PSA) was constructed based on dual-quenching of photocurrent from CdSe sensitized TiO_2 electrode by gold nanoparticles decorated dopamine–melanin nanospheres (AuNPs-Dpa-melanin CNSs). In this proposal, CdSe sensitized TiO_2 was used as photoelectrochemical matrix and the functional AuNPs-Dpa-melanin CNSs were used as signal quenching element. The dual quenching of the gold nanoparticles decorated Dpa-melanin CNSs to the CdSe sensitized TiO_2 was achieved as follows: (i) the strong energy transfer between the CdSe quantum dots (QDs) and Au NPs diminishes the photocurrent signal of CdSe QDs; (ii) the steric hindrance of AuNPs-Dpa-melanin CNSs partly obstructs the diffusion of the electron donor, i.e. ascorbic acid, to the surface of photoelectrode, which make the depleting efficiency of the photogenerated holes decrease, leading to a declined photocurrent intensity. On the basis of the dual quenching effect of AuNPs-Dpa-melanin CNSs, a competitive immunosensing platform for PSA was designed upon the specific binding of anti-PSA to PSA and PSA functionalized AuNPs-Dpa-melanin CNSs conjugates. This proposed immunosensor possesses wide linear range from 1.0×10^{-11} g mL^{-1} to 1.0×10^{-7} g mL^{-1} with the detection limit of 2.7 pg mL^{-1}. Moreover, the applicability of the present method was demonstrated in the determination of PSA in human serum. The strategy creates new paradigms for PSA and other tumor markers detection and demonstrates high sensitivity, good specificity, and satisfied applicability in complex biological samples.

1. Introduction

Photoelectrochemical (PEC) technique, with features such as simple devices, low cost and simple operation, and high sensitivity, is becoming an innovative and powerful analytical method for bioanalysis. To date, PEC technique has been applied for the determination various target analytes including DNA, protein, metal ions and cells (Zhao et al., 2014a, 2014b, 2015, 2016). The consistent detection principle of PEC biosensors is that the photocurrent change could be produced by the biological interactions between the various recognition elements and their corresponding targets. The photocurrent changes in the detection process often relay on the steric hindrance effects (Wang et al., 2009), the consumption/generation of coreactant based on enzymatic reactions (Cao et al., 2015; Wang et al., 2014b) and the Förster resonance energy transfer (FRET) between semiconductor nanocrystals and metallic nanoparticles (Shen et al., 2015; Xu et al., 2016; Zhao et al., 2012). Among various methods, the signal quenching strategies via the consumption of the coreactant, steric hindrance effect, or exciton energy transfer (EET) have been usually utilized for the construction of PEC biosensors. For example, Wang et al. developed a label-free PEC immunoassay for α-fetoprotein detection based on the steric hindrance of the immunocomplex for ascorbic acid to the surface of CdS (Wang et al., 2009). By monitoring the formation or consumption of hydrogen peroxide as coreactant, quantum dots functionalized porous ZnO nanosheets-based PEC platform has been designed for DNA detection (Wang et al., 2014b). Based on the strong EET effect between Au NPs and CdSe quantum dots (QDs), a highly sensitive DNA methyltransferase activity and inhibitor screening PEC

* Corresponding authors at: College of Chemistry and Chemical Engineering, Xinyang Normal University, Xinyang 46400, China.
E-mail addresses: jtcao11@163.com, jtcao11@163.com (J.-T. Cao), liuym9518@sina.com (Y.-M. Liu).

http://dx.doi.org/10.1016/j.bios.2016.12.043
Received 9 October 2016; Received in revised form 3 December 2016; Accepted 16 December 2016
Available online 18 December 2016
0956-5663/

assay has been developed (Shen et al., 2015). Summarized from these examples, single signal change path was always adopted. It would be deduced that the combination of two or more these signal change paths might yield synergetic effect to the PEC system, which might greatly improve the detection sensitivity.

Dopamine-melanin colloidal nanospheres (Dpa-melanin CNSs) with the advantages of excellent compatibility and biodegradability are appealing materials for the construction of sensing interface due to its rich surface-functional groups (–OH, $–NH_2$) for easily conjugation with some interesting molecules. Up to now, the Dpa-melanin CNSs have been exploited in the field of fluorescent (Xie et al., 2015), chemiluminescent (Wang et al., 2016), electrochemical (Wang et al., 2014a), and ECL (Liu et al., 2014) detection. In our previous work, Dpa-melanin CNSs immobilized with $Ru(bpy)_3^{2+}$ were used as an ECL tag for sensitive thrombin detection (Liu et al., 2014). The Dpa-melanin with large surface area could enrich a large number of luminophore reagent such as $Ru(bpy)_3^{2+}$ on its surface and thus could produce a strong ECL response. Inspired by this ingenious idea, a large amount of gold nanoparticles (AuNPs) could be also immobilized on the surface of Dpa-melanin CNSs. Compared with the bioprobes that one bioprobe labeled with one single AuNP (Shen et al., 2015), the AuNPs coated Dpa-melanin CNSs would become more efficient energy acceptors in the EET of the PEC system. How about the AuNPs coated Dpa-melanin CNSs working in the PEC assay?

Herein, a novel competitive PEC immunosensor for protein detection was developed based on dual signal quenching strategy. The Dpa-melanin CNSs were facilely synthesized from dopamine hydrochloride in an alkaline environment and the AuNPs-Dpa-melanin CNSs were prepared by *in situ* growth of AuNPs on Dpa-melanin CNSs. To fabricate the immunosensor, TiO_2, PDDA, CdSe QDs, antibody (Ab), were stepwise assembled on an indium tin oxide (ITO) electrode as depicted in Scheme 1. Prostate specific antigen (PSA), a valuable premier tumor marker for detecting early stage prostate cancer or other prostate disorders, was used as a model protein in this work. In the absence of PSA, the PSA-AuNPs-Dpa-melanin CNSs conjugates specifically bound with Ab specific for PSA on the electrode. The bound of PSA-AuNPs-Dpa-melanin CNSs could induce an obvious decrease of photocurrent signal by both the EET effect between CdSe QDs and AuNPs and the steric hindrance of Dpa-melanin CNSs. In the presence of PSA, the competitive interaction of PSA and PSA-AuNPs-Dpa-melanin CNSs with the Ab on the electrode was occurred. In this state, the amount of PSA-AuNPs-Dpa-melanin CNSs conjugates bound on the electrode decreased, producing an increased photocurrent signal compared to the electrode only with PSA-AuNPs-Dpa-melanin CNSs incubation. Under the optimum conditions, the immunosensor exhibits excellent performance for PSA detection. Furthermore, the application of the proposed sensing strategy was demonstrated by determination the concentration of PSA in complex biological samples.

2. Experimental

2.1. Materials and reagents

Prostate specific antigen (PSA, L2C001) standards and mouse monoclonal PSA antibody (clone L1C00401, capture antibody, Ab) were purchased from Shanghai Linc-Bio Science Co., Ltd. (Shanghai, China). TiO_2 powder was from the Degussa Co. (P25, Germany). Hyrogen tetra chloroaurate(III) trihydrate ($HAuCl_4·3H_2O$), ascorbic acid (AA), cadmium chloride ($CdCl_2·2.5H_2O$) and sodium borohydride ($NaBH_4$) were obtained from Shanghai Reagent Company (Shanghai, China). Human serum albumin (HSA), human immunoglobulin (hIgG), bovine serum albumin (BSA), and thrombin (TB) were from Shanghai Solarbio Bioscience & Technology Co., Ltd. (Seebio Biotechnology). Poly(diallyldimethylammonium chloride) (PDDA; 20%, w/w in water, MW=200,000–350,000), selenium powder (Se), thioglycolic acid (TGA), *N*-(3-Dimethylaminopropyl)-*N*-ethyl-carbodiimide hydrochloride (EDC), *N*-hydroxysuccinimide (NHS) were purchased from Sigma-Aldrich. Other chemicals were of analytical reagent grade and used as received. All aqueous solutions were prepared using pure water (18.2 MΩ·cm, ultrapure water system from Aike Water Treatment Solution Provider, China).

2.2. Apparatus

PEC signal was detected by the home-made PEC system equipped with a 500 W Xe lamp. Photocurrent was measured on a RST5200 electrochemical workstation (Zhengzhou Shiruisi Technology Co., Ltd., China) with a three-electrode system: a modified ITO electrode with a geometrical area of 0.25 cm^2 as the working electrode, a Pt wire as the auxiliary electrode and a saturated Ag/AgCl electrode as the reference electrode. A 0.01 M phosphate buffer solution (PBS, pH 7.4) containing 0.1 M AA was used as the electrolyte for photocurrent measurements.

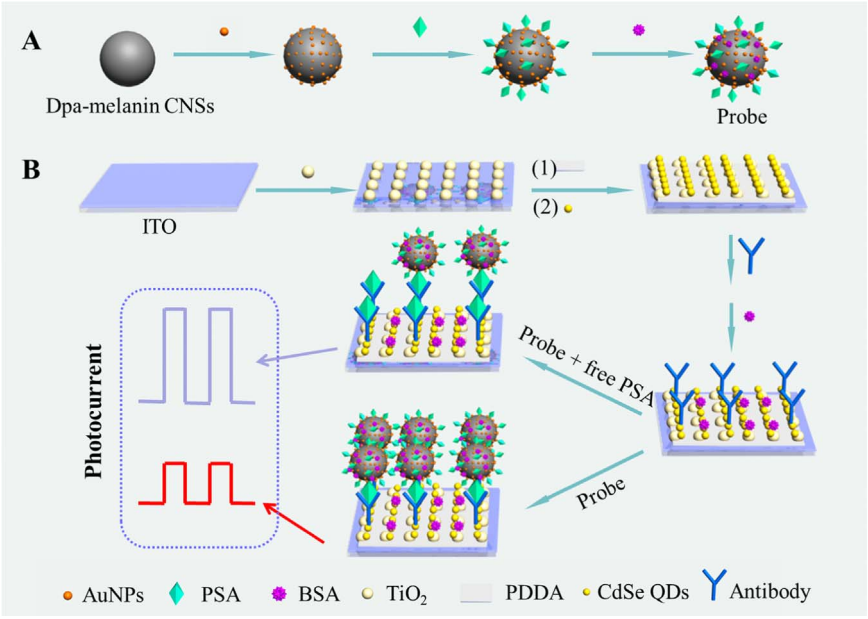

Scheme 1. (A) The preparation of the probe. (B) The fabrication procedure of the immunosensor.

Cyclic voltammetry (CV) and electrochemical impedance spectroscopy (EIS) were also performed on RST5200 electrochemical workstation with a three electrode system in KCl solution (0.1 M) containing 5 mM $K_4[Fe(CN)_6]/K_3[Fe(CN)_6]$ (1:1). The UV–vis absorption spectrum was recorded on an UVmini-1240 UV–vis spectrophotometer (Shimadzu, Japan). Photoluminescence (PL) signal was measured using a RF-5301PC fluorescence spectrometer (Shimadzu Co., Japan). Scanning electron microscopy (SEM) and energy dispersive spectrometer (EDS) image were obtained by S-4800 (Hitachi, Tokyo, Japan). High resolution transmission electron microscope (HRTEM) image was recorded by JEM-2100F (JEOL Ltd., Tokyo, Japan).

2.3. Preparation of CdSe QDs

The water-soluble TGA capped CdSe QDs were prepared according to the literature (Liu et al., 2008). Briefly, NaHSe precursor solution was firstly obtained from the reaction of Se powder and $NaBH_4$ solution under nitrogen atmosphere. After 50 mL of 2 mM $CdCl_2$ solution was mixed with 20 μL of TGA (pH=10) and bubbled with highly pure N_2 for 30 min 0.7 mL of 70 mM freshly prepared NaHSe was injected into the mixture to obtain a clear, lightly yellow solution. The resulting solution was kept at 100 °C and refluxed for 4 h under N_2 protection, and finally the desired TGA-modified CdSe QDs solution

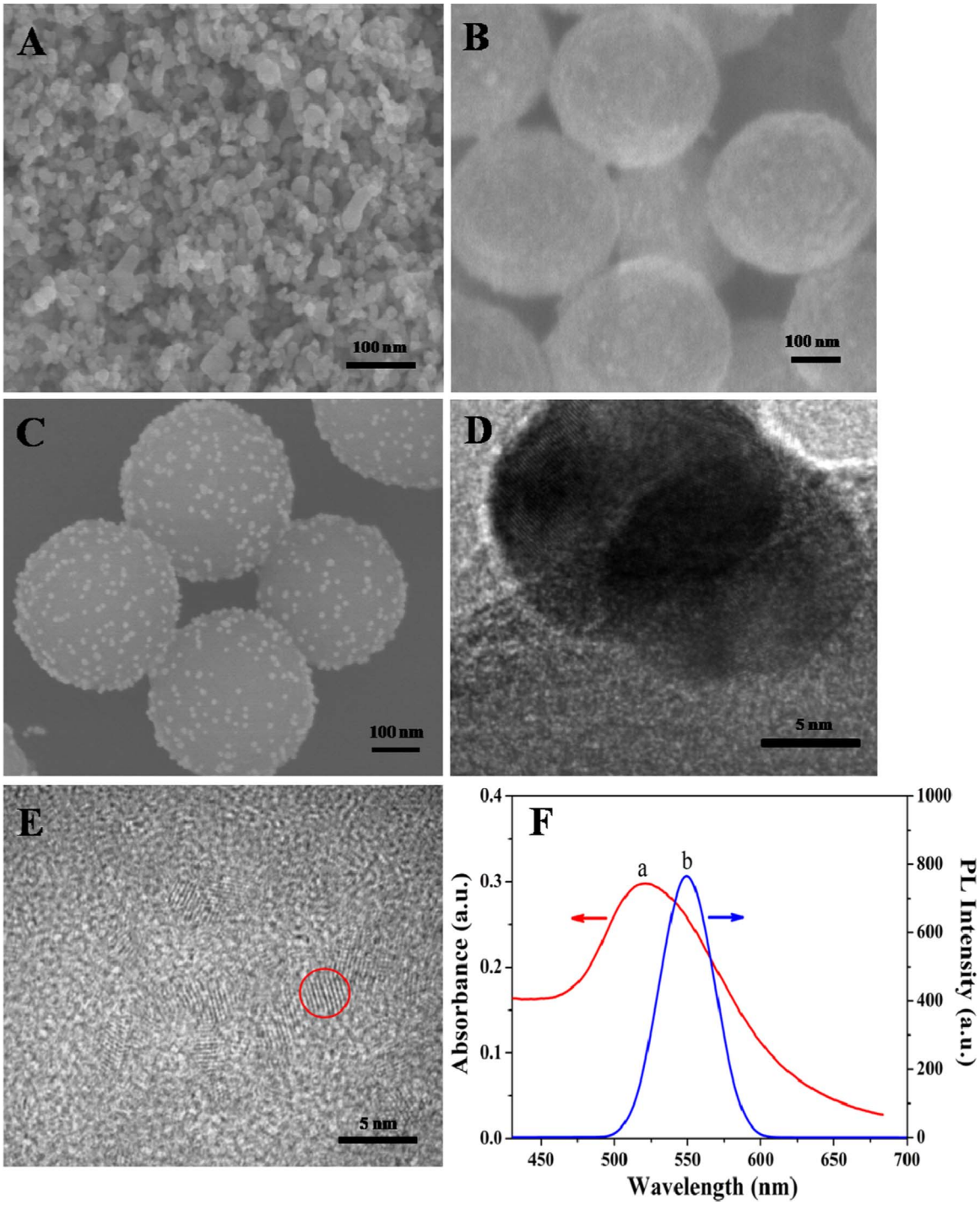

Fig. 1. SEM images of (A) TiO_2 on the surface of ITO; (B) Dpa-melanin CNSs; (C) AuNPs-Dpa-melanin CNSs; (D) HRTEM images of the AuNPs-Dpa-melanin CNSs and (E) CdSe QDs; (F) absorption spectrum of Au NPs (a) and PL emission spectrum of the CdSe QDs (b).

was obtained.

2.4. Synthesis of AuNPs-Dpa-melanin CNSs and PSA-AuNPs-Dpa-melanin CNSs conjugates

Dpa-melanin CNSs were prepared according to the reported method (Liu et al., 2013). AuNPs-Dpa-melanin CNSs were synthesized as follows. Firstly, 1 mg mL^{-1} Dpa-melanin CNSs was mixed with 380 μL of 0.1% $HAuCl_4{\cdot}3H_2O$ under stirring for 5 min. Then, 0.5 mM of 400 μL AA was rapidly added into the mixture solution and stirred for 4 min. The resultant solution was centrifuged and washed with pure water for three times. AuNPs-Dpa-melanin CNSs precipitate was resuspended in 0.01 M PBS. The synthetic procedure of PSA-AuNPs-Dpa-melanin CNSs conjugates was described as below. 25 μL of 80 μg mL^{-1} PSA was added in AuNPs-Dpa-melanin CNSs and stirred at 30 °C for 2 h. After being centrifuged and washed with 0.01 M PBS several times, the desired AuNPs-Dpa-melanin CNSs conjugates were acquired and dispersed in 1 mL PBST (0.01 M PBS dissolved in 0.05% Tween 20) containing 0.1% BSA and stored at 4 °C.

2.5. Construction of photoelectrochemical immunosensor

The ITO electrode was cleaned with chemical detergent solution, acetone, NaOH (1.0 M) in ethanol/water mixture (1:1, *v*/*v*), and water, respectively. Firstly, 20 μL of 1 mg mL^{-1} TiO_2 suspension was dropped onto the clear ITO electrode. After drying in air, the electrode was sintered at 450 °C for 30 min under ambient atmosphere. The CdSe QDs/TiO_2/ITO electrode was fabricated by alternately dipping of the as-obtained TiO_2/ITO into a solution of positively charged PDDA for 30 min and the negative charged TGA-modified CdSe QDs for 1 h, respectively. After that, CdSe QDs/TiO_2/ITO electrode was treated with 20 μL of aqueous solution containing 20 mg mL^{-1} EDC and 10 mg mL^{-1} NHS for 1 h to activate the COOH groups on the surface of the CdSe QDs. Next, Ab to PSA was casted onto the resulting electrode surface at 4 °C for 12 h. Finally, the Ab/CdSe QDs/TiO_2/ITO electrode was incubated with 2% BSA at 37 °C for 1 h to block nonspecific binding sites. For PSA detection, 20 μL of mixed solution containing 10 μL PSA-AuNPs-Dpa-melanin CNSs and 10 μL different concentrations of PSA were dropped on the modified electrode at 37 °C for 50 min.

3. Results and discussion

3.1. Characterization of TiO_2, CdSe QDs and AuNPs-Dpa-melanin CNSs

To acquire the feature of TiO_2 and confirm the successful synthesis of AuNPs-Dpa-melanin CNSs and CdSe QDs, SEM and HRTEM were performed and the micrographs were displayed in Fig. 1. As shown in Fig. 1A, a large number of TiO_2 nanoparticles have been formed on ITO electrode surface and the mesoporous TiO_2 film is beneficial to load more amount of CdSe QDs. Fig. 1B is the SEM image of Dpa-melanin CNSs. It can be seen that the surface of Dpa-melanin CNSs is rough and the average size of the nanospheres is about 300 nm (Fig. 1B). After the Dpa-melanin CNSs were functionalized with AuNPs by *in situ* growth method, as shown in Fig. 1C, the AuNPs with the size of 12 ± 2 nm were scattered uniformly on the surface of Dpa-melanin CNSs. Also, the HRTEM view shown in Fig. 1D gives the similar result that the AuNPs with the size of about 12 nm were immobilized on the surface of Dpa-melanin CNSs. The typical HRTEM image of CdSe QDs shows that the QDs are sufficiently monodisperse and well separated with a mean size of 3 nm.

The EDS spectra of the TiO_2/ITO, CdSe/TiO_2/ITO electrodes, Dpa-melanin CNSs, and AuNPs-Dpa-melanin CNSs nanoparticles have also been performed and the results were shown in Fig. S1. It can be seen from Fig. S1A that only Ti and O elements appeared, illustrating the

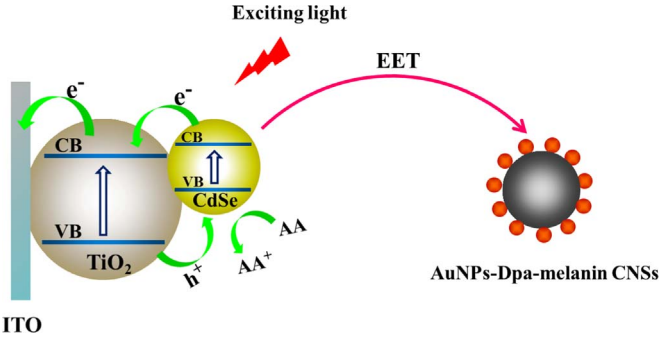

Scheme 2. PEC mechanism of the immunosensor.

TiO_2 were pure. And the existence of CdSe QDs can be verified in Fig. S1B. The elements of Ti, O, Cd and Se existed in Fig. S1B suggested that CdSe QDs were successfully assembled on TiO_2 electrode. Compare to Dpa-melanin CNSs (Fig. S1C), Au element appeared in Fig. S1D, which means the AuNPs-Dpa-melanin CNSs were successfully synthesized.

To achieve EET, the spectra overlap between the emission spectra of the CdSe QDs and absorption spectra of AuNPs is essential. As can be seen from Fig. 1F, the PL emission of the CdSe QDs has a considerable spectral overlap with the absorption of the AuNPs, which is favorable for the inducement of the surface plasmon resonance (SPR) of the AuNPs. The SPR affects the subsequent interparticle energy transfer and thus reduces the photocurrent response (in Scheme 2).

3.2. Electrochemical and photoelectrochemical behaviors of the immunosensor

The stepwise modification process of the immunosensor was verified by CV measurements. Fig. 2A displays the CV curves of the electrodes at different fabrication steps in the presence of 5.0 mM $K_3[Fe(CN)_6]/K_4[Fe(CN)_6]$ (1:1) containing 0.1 M KCl. Compared with the bare ITO (curve a), the peak current of TiO_2 modified ITO decreased (curve b) owing to the low conductivity of TiO_2 semiconductors. When the electrode was modified with PDDA and CdSe QDs sequentially, gradually decreased peak currents were found (curve c), due to the insulating effect of PDDA and weak electrical conductivity of CdSe QDs. With the Ab and BSA assembled on the electrode, the peak currents decreased (curve d and e). After incubation of the modified electrode with the probe, the CV response of the electrode further decreased apparently. This is attributed to the fact that the PSA-AuNPs-Dpa-melanin CNSs conjugates with poor conductivity could hinder the electron transfer (curve f). The assembly process of the immunosensor was also tested with EIS method. As shown in Fig. 2B, the results of EIS data are in accordance with the CV data, confirming the successful construction of immunosensor.

PEC behaviors of the electrode at the assembly process were also investigated and the results were depicted in Fig. 3A. It can be seen that no photocurrent response was observed for the bare ITO (curve a). After dropped TiO_2 suspension onto the electrode, the photocurrent intensity increased (curve b), which shows good performance of TiO_2 for the construction of PEC biosensor. With the modification process, the photocurrent intensity increased sharply for CdSe/TiO_2 modified electrode (curve c), because of the sensitization effect of CdSe QDs. Later on, the photocurrents of the electrodes sequentially modified by Ab (curve d) and BSA (curve e) declined because these protein molecules could hinder the diffusion of AA to the surface of CdSe/TiO_2/ITO electrode. The photocurrent further decreased acutely after incubation of the modified electrode with the probe (curve f). This acute decrease could be ascribed to both the steric hindrance effect of the Dpa-melanin CNS and the efficient EET between the AuNPs and CdSe QDs. However, an enhanced photocurrent response was observed

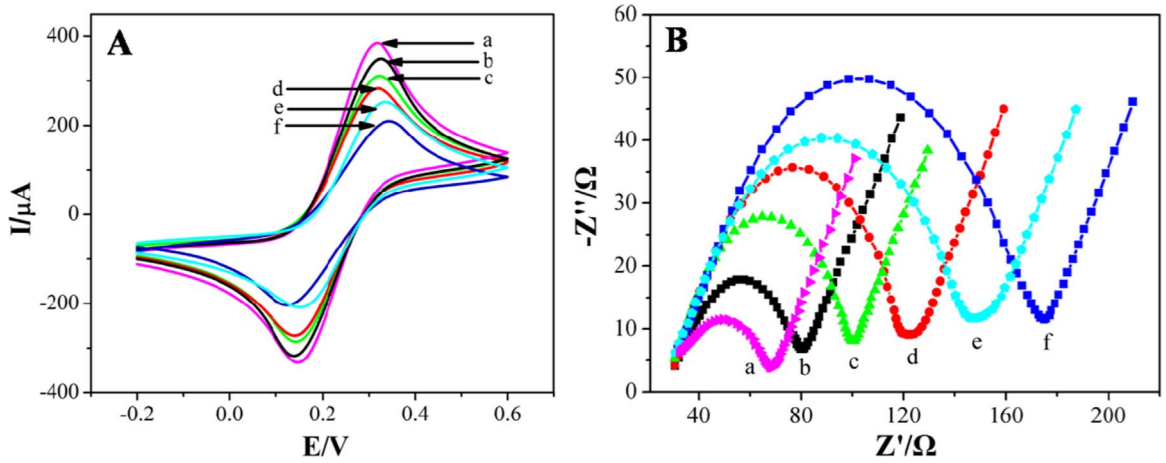

Fig. 2. (A) CVs and (B) EIS of electrodes at different stages in 5.0 mM $K_3[Fe(CN)_6]/K_4[Fe(CN)_6]$ (1:1) mixture containing 0.1 M KCl: (a) bare ITO; (b) TiO_2/ITO; (c) CdSe/PDDA/TiO_2/ITO; (d) Ab/CdSe/PDDA/TiO_2/ITO; (e) BSA/Ab/CdSe/PDDA/TiO_2/ITO and (f) probe/BSA/Ab/CdSe/PDDA/TiO_2/ITO.

in the presence of PSA (curve g), due to a competition in the free PSA and the PSA-AuNPs-Dpa-melanin CNSs conjugates toward Ab on the electrode, the free PSA with smaller size bound with the Ab more facilely than the probe with relative large size, resulting in the amount of PEC quenching probes (PSA-AuNPs-Dpa-melanin CNSs) immobilized on the electrode decreased.

In order to estimate the effect of the AuNPs-Dpa-melanin CNSs on PEC signal, two sensors, PSA-Dpa-melanin CNSs/BSA/Ab/CdSe/PDDA/TiO_2/ITO (curve b in Fig. 3B) and PSA-AuNPs-Dpa-melanin CNSs/BSA/Ab/CdSe/PDDA/TiO_2/ITO (curve c), were fabricated and compared with BSA/Ab/CdSe/PDDA/TiO_2/ITO (curve a) under the same experimental conditions. The results reveal that the PEC intensity of the probe with Au-coating is lower than that without Au-coating, indicating that the probe with Au coating could produce more efficient quenching effect. The great quenching effect from the AuNPs-Dpa-melanin CNSs further substantiates the synergistic effect of both the steric hindrance effect of the Dpa-melanin CNS and the efficient EET between AuNPs and CdSe QDs.

3.3. Optimization of experimental conditions

The present strategy is based on the competitive binding of Ab with free PSA and the quenching probe. The incubation temperature and time for the Ab-PSA interaction greatly influence the sensitivity of the immunosensor. The effect of incubation temperature ranged from 25 °C to 50 °C was tested. As show in Fig. S2A, the photocurrent intensity decreased with the rising of temperature from 25 °C to 37 °C and then increased from 37 °C to 50 °C. Therefore, the best binding temperature for Ab-PSA interaction is 37 °C. To screen the proper incubation time on the photocurrent response, the incubation time from 0 to 50 min was examined. As can be seen from Fig. S2B, the photocurrent intensity gradually decreased with the increasing incubation time until 50 min and the incubation time longer than 50 min did not produce further signal change. So, 50 min was chosen.

3.4. Analytical performances of photoelectrochemical biosensor

To track the relationship between the photocurrent and the content of PSA, a series of PSA concentrations from 1.0×10^{-12} to 5.0×10^{-6} g mL^{-1} were tested. The results presented in Fig. 4 shows that the photocurrent response of the immunosensor is proportional to the logarithm of the PSA concentration in the range of 1.0×10^{-11} to 1.0×10^{-7} g mL^{-1} with the regression equation of I (μA)=166.45+8.41 log C_{PSA} (g mL^{-1}) with the correlation coefficient of 0.995. The limit of detection (LOD) was experimentally found to be 2.7 pg mL^{-1}, which is lower than 0.2 ng mL^{-1} for an electrochemical senor (Zhao et al., 2010), 0.1 ng mL^{-1} for an ECL method (Yang et al., 2015), 27 pg mL^{-1} for a fluorescence detection (Xu et al., 2017), 0.4 and 0.08 ng mL^{-1} for colorimetric and fluorescence assay in a fluoropolymer microfluidic device, respectively (Barbosa et al., 2015), and comparable to a

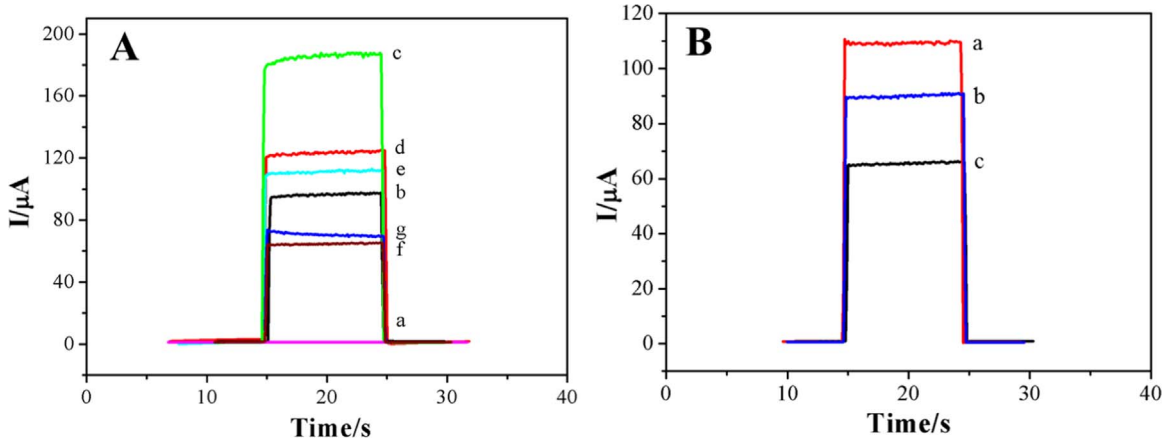

Fig. 3. (A) Photocurrent responses of the modified ITO electrodes in 0.1 M PBS (pH 7.4) containing 0.1 M AA: (a) bare ITO; (b) TiO_2/ITO; (c) CdSe/PDDA/TiO_2/ITO; (d) Ab/CdSe/PDDA/TiO_2/ITO; (e) BSA/Ab/CdSe/PDDA/TiO_2/ITO; (f, g) BSA/Ab/CdSe/PDDA/TiO_2/ITO electrode after incubation with 10 μL of PSA-AuNPs-Dpa-melanin CNSs bioconjugates and 10 μL of PBS (f) or 10 μL of PSA-AuNPs-Dpa-melanin CNSs bioconjugates and 10 μL of 1.0×10^{-11} g mL^{-1} PSA (g), which were measured in 0.01 M PBS (pH 7.4) containing 0.1 M AA. (B) Photocurrent responses of BSA/Ab/CdSe/PDDA/TiO_2/ITO (a); after incubation with 10 μL of PSA-Dpa-melanin CNSs bioconjugates and 10 μL of PBS (b) or incubation with 10 μL of PSA-Au-Dpa-melanin CNSs bioconjugates and 10 μL of PBS (c).

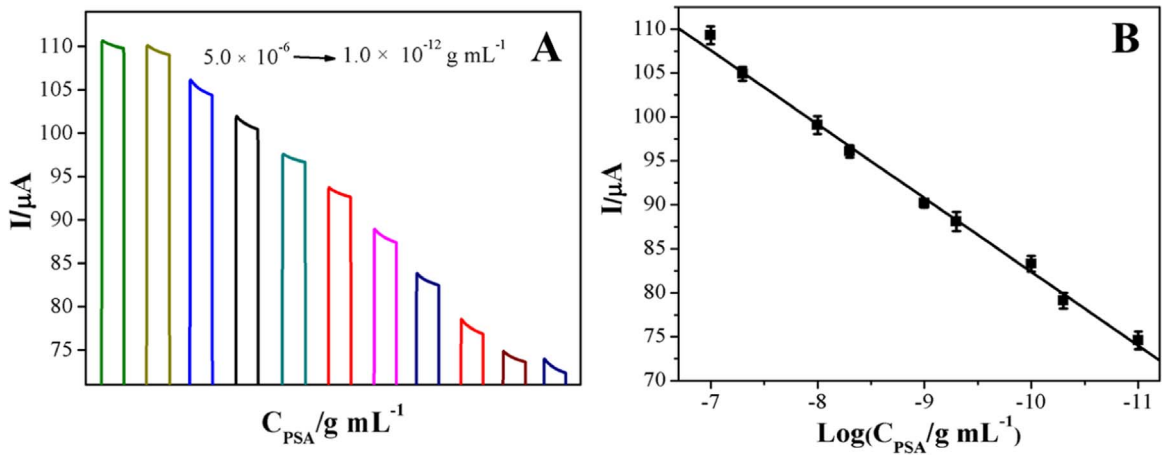

Fig. 4. (A) Photocurrent response of the different concentration of PSA. (B) The linear calibration curve of PSA. Error bars represent standard deviations of measurements (n=3).

chemiluminesence excited PEC biosensing strategy with a detection limit of 3 pg mL^{-1} (Tu et al., 2012). The linear response range was also wider than those electrochemical (0.5–40 ng mL^{-1}, Zhao et al. (2010)), ECL (0.5–40 ng mL^{-1}, Yang et al., 2015), fluorescent (0.1–100 ng mL^{-1}, Xu et al. (2017)), colorimetric and fluorescent double-check strategy (0.9–60 ng mL^{-1}, Barbosa et al. (2015)), and PEC detection (0.01–80 ng mL^{-1}, Tu et al., 2012). The data exhibits the superiority of the present immunosensor over some earlier reported methods for the detection limit and linear range. The wide linear range and low LOD will broaden the practical application of the present method.

3.5. Selectivity, reproducibility, and stability of the biosensor

To evaluate the selectivity of the immunesensor, the photocurrent responses of other proteins including HSA, hIgG, and TB were recorded. As shown in Fig. S3, the photocurrents of the interfering proteins are nearly the same as that in the blank solution. Furthermore, no significant change of photocurrent could be observed as for the mixture containing 40 mg mL^{-1} HSA, 20 mg mL^{-1} hIgG, 10 μg mL^{-1} TB, and 0.1 ng mL^{-1} PSA, comparing with the result acquired in the presence of PSA only. The results reveal that the prepared immunosensor has good selectivity.

The reproducibility of the immunoassay was investigated on the basis of the relative standard deviation (RSD) for the intra-assay and inter-assay. The intra-assay was performed by measuring PSA five times at concentrations of 0.1 ng mL^{-1} and 100 ng mL^{-1} which yielded RSD values of 2.5% and 4.1%, respectively. The inter-assay was determined by assaying PSA at the same concentration using five sensing electrodes prepared under identical conditions, where the RSD values were 4.2% and 6.1%, respectively. In addition, the stability of the designed immunesensor was also evaluated by measuring its photocurrent response at three-week period storage at 4 °C. The photocurrent responses for both 0.1 ng mL^{-1} and 100 ng mL^{-1} PSA had no obvious change after storage for three weeks, showing good stability and detection reliability.

3.6. Application in complex biological samples

In order to validate the feasibility, the designed biosensor was utilized to determine PSA in complex biological samples. Nine human serum samples from Xinyang Central Hospital were measured by the immunosensor and ROCHE ECL analyzer employed in Xinyang Central Hospital as the reference. The serum samples used were not diluted and the analytical results were listed in Table S1. The relative errors between this work and the reference method are less than 8.4%, and the RSDs are no more than 6.2%, which shows that the matrix effect has no obvious influence on the response to PSA.

4. Conclusions

In summary, a highly sensitive PEC immunosensor for PSA detection has been demonstrated based on the dual quenching of functionalized AuNPs-Dpa-melanin CNSs toward the CdSe sensitized TiO_2 electrode. As photoelectrochemical matrix of the immunosensor, $CdSe/TiO_2$ sensitization structure could greatly enhance the photocurrent thanks to the sensitization effect of CdSe QDs. As signal quenching element, PSA-AuNPs-Dpa-melanin CNSs conjugates could efficiently weaken the photocurrent intensity due to synergistic quenching effects from the strong energy transfer between the CdSe QDs and Au NPs and the steric hindrance of the nanoprobes. Integrating the fine PEC performance of the $CdSe/TiO_2$ sensitization structure with the superior quenching effect of the AuNPs-Dpa-melanin CNSs conjugates together, the well-established PEC immunosensing platform exhibits a highly sensitive response to PSA with good selectivity and satisfied stability. Moreover, the applicability of PSA detection in human serum suggests that this new PEC platform has a great promise for potential applications in the detection of disease-related biomarkers with low levels.

Acknowledgements

This work was supported by the National Natural Science Foundation of China (21375114, 21405129, and 21675136), Plan for Scientific Innovation Talent of Henan Province, State Key Laboratory of Analytical Chemistry for Life Science (SKLACLS1419), and Nanhu Young Scholar Supporting Program of XYNU.

Appendix A. Supplementary material

Supplementary material associated with this article can be found in the online version at doi:10.1016/j.bios.2016.12.043.

References

Barbosa, A.I., Gehlot, P., Sidapra, K., Edwards, A.D., Reis, N.M., 2015. Biosens. Bioelectron. 70, 5–14.
Cao, J.T., Zhang, J.J., Gong, Y., Ruan, X.J., Liu, Y.M., Chen, Y.H., Ren, S.W., 2015. J. Electroanal. Chem. 759, 46–50.
Liu, X., Cheng, L., Lei, J., Ju, H., 2008. Analyst 133, 1161–1163.
Liu, Y., Ai, K., Liu, J., Deng, M., He, Y., Lu, L., 2013. Adv. Mater. 25, 1353–1359.
Liu, Y.M., Zhang, J.J., Shi, G.F., Zhou, M., Liu, Y.Y., Huang, K.J., Chen, Y.H., 2014. Electrochim. Acta 129, 222–228.
Shen, Q.M., Han, L., Fan, G.C., Abdel-Halim, E.S., Jiang, L.P., Zhu, J.J., 2015. Biosens. Bioelectron. 64, 449–455.
Tu, W.W., Wang, W.J., Lei, J.P., Deng, S.Y., Ju, H.X., 2012. Chem. Commun. 48, 6535–6537.

Wang, G.L., Xu, J.J., Chen, H.Y., Fu, S.Z., 2009. Biosens. Bioelectron. 25, 791–796.
Wang, H.B., Zhang, H.D., Xu, L.L., Gan, T., Huang, K.J., Liu, Y.M., 2014a. J. Solid State Electr. 18, 2435–2442.
Wang, Q., Yin, B.C., Ye, B.C., 2016. Biosens. Bioelectron. 80, 366–372.
Wang, W., Hao, Q., Wang, W., Bao, L., Lei, J., Wang, Q., Ju, H., 2014b. Nanoscale 6, 2710–2717.
Xu, D.D., Deng, Y.L., Li, C.Y., Lin, Y., Tang, H.W., 2017. Biosens. Bioelectron. 87, 881–887.
Xu, F., Zhu, Y.C., Ma, Z.Y., Zhao, W.W., Xu, J.J., Chen, H.Y., 2016. Chem. Commun. 52, 3034–3037.
Xie, Y., Lin, X., Huang, Y., Pan, R., Zhu, Z., Zhou, L., Yang, C.J., 2015. Chem. Commun. 51, 2156–2158.
Yang, H.Y., Zhe, J.L., Shan, M., Li, C.C., Qi, H.L., Gao, Q., Wang, J.Y., Zhang, C.X., 2015. Anal. Chim. Acta 863, 1–8.
Zhao, N., He, Y.Q., Mao, X., Sun, Y.H., Zhang, X.B., Li, C.Z., Lin, Y.H., Liu, G.D., 2010. Electrochem. Commun. 12, 471–474.
Zhao, W.W., Xiong, M., Li, X.R., Xu, J.J., Chen, H.Y., 2014a. Electrochem. Commun. 38, 40–43.
Zhao, W.W., Xu, J.J., Chen, H.Y., 2016. Anal. Chem. 82, 307–315.
Zhao, W.W., Xu, J.J., Chen, H.Y., 2014b. Chem. Rev. 114, 7421–7441.
Zhao, W.W., Xu, J.J., Chen, H.Y., 2015. Chem. Soc. Rev. 44, 729–741.
Zhao, W.W., Yu, P.P., Shan, Y., Wang, J., Xu, J.J., Chen, H.Y., 2012. Anal. Chem. 84, 6535–6537.